Neurobiology of Disease 73 (2015) 366–376

Contents lists available at ScienceDirect

Neurobiology of Disease

journal homepage: www.elsevier.com/locate/ynbdi

Injured adult retinal axons with Pten and Socs3 co-deletion reform active synapses with suprachiasmatic neurons

Songshan Li [a,b,1], Qinghai He [a,b,1], Hao Wang [c], Xuming Tang [a,b], Kam Wing Ho [d], Xin Gao [a,b], Qian Zhang [a,b], Yang Shen [a,b], Annie Cheung [a], Francis Wong [a,b], Yung Hou Wong [a], Nancy Y. Ip [a,b], Liwen Jiang [c], Wing Ho Yung [d], Kai Liu [a,b,*]

[a] Division of Life Science, State Key Laboratory of Molecular Neuroscience, School of Science and Institute for Advance Study, The Hong Kong University of Science and Technology, Clear Water Bay, Kowloon, Hong Kong, China
[b] Center of Systems Biology and Human Health, School of Science and Institute for Advance Study, The Hong Kong University of Science and Technology, Clear Water Bay, Kowloon, Hong Kong, China
[c] School of Life Sciences, Centre for Cell and Developmental Biology and State Key Laboratory of Agrobiotechnology, Faculty of Medicine, The Chinese University of Hong Kong, Shatin, New Territories, Hong Kong, China
[d] School of Biomedical Sciences, Faculty of Medicine, The Chinese University of Hong Kong, Shatin, New Territories, Hong Kong, China

ARTICLE INFO

Article history:
Received 16 April 2014
Revised 1 September 2014
Accepted 12 September 2014
Available online 16 October 2014

Keywords:
Axon regeneration and rewiring
Intrinsic mechanisms
Pre-chiasm lesion
Retinal ganglion cells
Suprachiasmatic nucleus

ABSTRACT

Despite advances in promoting axonal regeneration after adult central nervous system injury, elicitation of a large number of lesion-passing axons reform active synaptic connections with natural target neurons remains limited. By deleting both *Pten* and *Socs3* in retinal ganglion cells, we report that optic nerve axons after prechiasm lesion robustly reinnervate the hypothalamus, form new synapses with neurons in the suprachiasmatic nucleus (SCN), and re-integrate with the existing circuitry. Photic or electric stimulation of the retinal axons induces neuronal response in SCN. However both the innervation pattern and evoked responses are not completely restored by the regenerating axons, suggesting that combining with other strategies is necessary to overcome the defective rewiring. Our results support that boosting the intrinsic growth capacity in injured neurons promotes axonal reinnervation and rewiring.

Introduction

Injuries to the adult mammalian central nervous system (CNS) often result in permanent functional deficits. A primary reason for such deficits is the CNS's limited ability to rewire. Severed axons cannot regenerate and reconnect to their original targets. Failure of axonal regeneration has mainly been attributed to the neurons' diminished growth capacity and an inhibitory environment (Bradke et al., 2012; Filbin, 2006; Giger et al., 2010; Harel and Strittmatter, 2006; Liu et al., 2011; Schwab and Bartholdi, 1996; Zheng et al., 2006). In past decades, retinal ganglion cells (RGCs) have been studied extensively to discover both intrinsic and extrinsic molecular mechanisms hindering regeneration. Several strategies have been developed to promote regrowth after optic nerve injury (Aguayo et al., 1981; Dickendesher et al., 2013; Leon et al., 2000; Moore et al., 2009; Park et al., 2008; Smith et al., 2009; Sun et al., 2011; Winzeler et al., 2011). However, it is not entirely clear whether a large number of regenerating retinal axons can reinnervate appropriate target area, and form active connections with appropriate neurons at the synaptic level.

Early studies by manually connecting the transected optic nerve with the superior colliculus through a peripheral nerve graft to bypass the lesion demonstrated that regenerating axons are able to reform synapses and conduct electric activity (Keirstead et al., 1989). But only a small number of axons penetrate into the brain and terminate at the proximity of the insertion site (Carter et al., 1989), suggesting limited axon growth capacity of RGCs in the CNS environment. Boosting intrinsic growth capacity of RGCs by combining *Pten* deletion with either *Socs3* deletion, or Zymosan and a cAMP analog leads to robust and long-distance regeneration within the optic nerve after intraorbital crush (de Lima et al., 2012; Luo et al., 2013; Sun et al., 2011). However, only a few axons innervate the brain. The limited innervation could partially due to the long distance for axons to travel (6–7 mm), misguidance within the nerve, and dramatic RGC death months after lesion.

What if presenting regenerating axons with a nature target at a shorter distance? Can they find the path to innervate, and make active

* Corresponding author at: Division of Life Science, State Key Laboratory of Molecular Neuroscience, School of Science and Institute for Advance Study, The Hong Kong University of Science and Technology, Clear Water Bay, Kowloon, Hong Kong, China.
E-mail address: kailiu@ust.hk (K. Liu).
Available online on ScienceDirect (www.sciencedirect.com).
[1] These authors contributed equally to this work.

http://dx.doi.org/10.1016/j.nbd.2014.09.019
0969-9961/

connections with appropriate neurons? To test this hypothesis, we performed a pre-chiasm optic nerve lesion, at a distance approximately 2–3 mm to the suprachiasmatic nucleus (SCN), then examined whether deleting both *Pten* and *Socs3* in RGCs promotes axon reinnervation. Here we report the sharpening and maturation of the newly formed SCN-projecting arbors, the reformation of asymmetric excitatory synapses, and the existence of photonically and electrically active but functionally compromised synapse by regenerating axons after adult CNS injury.

Material and methods

Animal and surgery

All experimental procedures were performed in compliance with animal protocols approved by the Animal and Plant Care Facility at the Hong Kong University of Science and Technology. C57BL/6J mice or *Pten*$^{f/f}$;*Socs3*$^{f/f}$ double-floxed mice (Sun et al., 2011) were used in this study. For all the surgery procedures, mice were anesthetized with

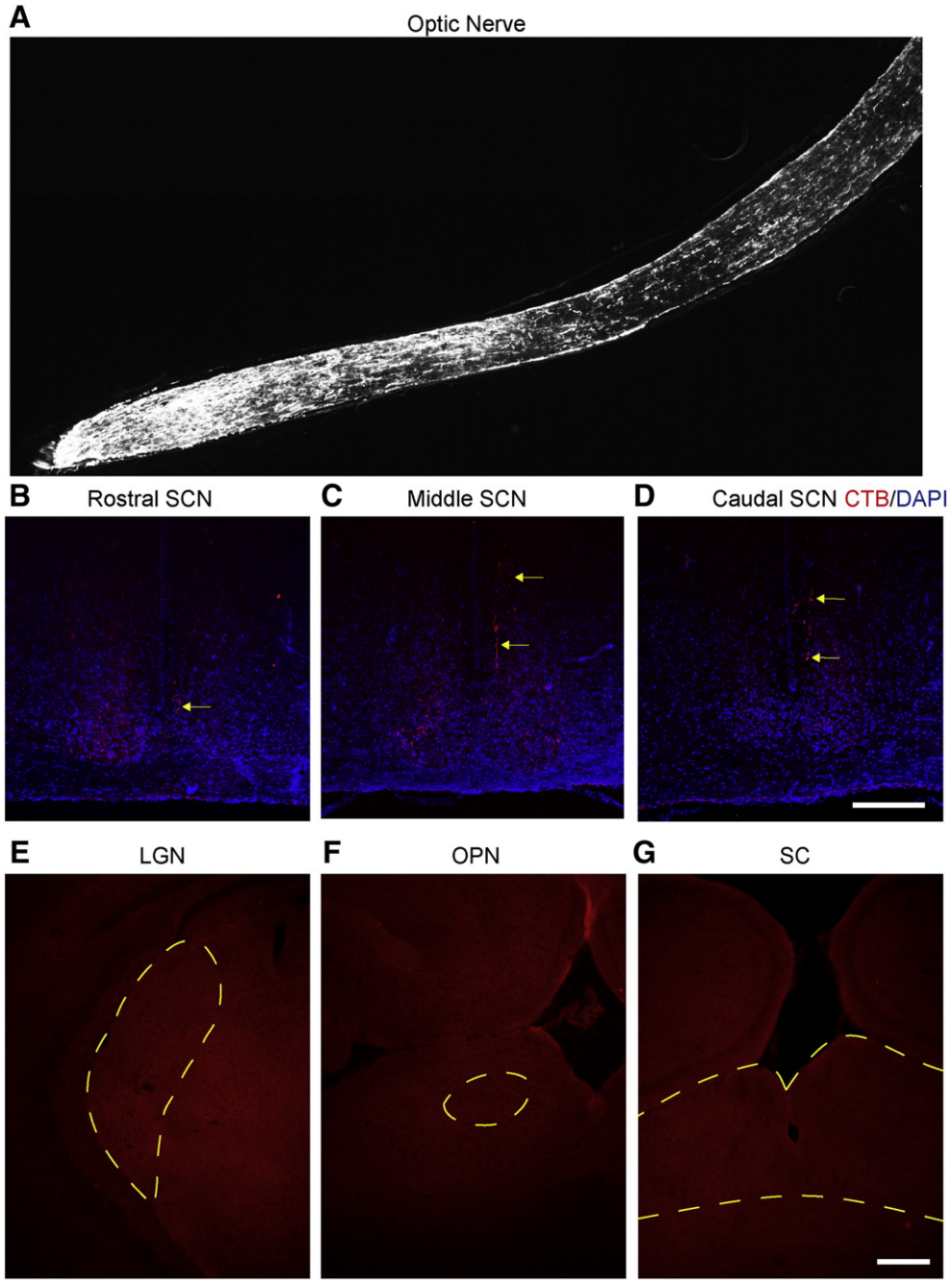

Fig. 1. Regeneration of RGC axons at 3 months after intraorbital optic nerve crush. (A) An image of the optic nerve showing CTB-labeled axons at 3 months after injury from a *Pten*$^{f/f}$;*Socs3*$^{f/f}$ mouse injected with AAV-Cre and CNTF. Inset shows the optic nerve projection and its major target nuclei. (B–D) A few axons were observed in the SCN area, indicated by arrows. (E–G) No axons were found in the LGN, OPN and SC. SCN: suprachiasmatic nucleus; LGN: lateral geniculate nucleus; OPN: olivary pretectal nucleus; SC: superior colliculus. Scale bar, A, B–D, 200 μm; E–G, 300 μm.

ketamine and xylazine, and received analgesic after operation. Eye ointment was applied to protect the cornea during and after surgery.

AAV injection

To delete both the Pten and Socs3 genes, 2 μl AAV-Cre or AAV-LacZ (titer ~10E12, Vector Biolabs) as control was injected into the vitreous body of 6–8 week old *Pten*$^{f/f}$;*Socs3*$^{f/f}$ double-floxed mice by glass micropipette conjugated to a Hamilton microsyringe, as described previously (Park et al., 2008). Three weeks after AAV injection, 1 μl CNTF (Prospec, 1 μg/μl) was intravitreally injected immediately, at 3 and 7 days after injury, and biweekly thereafter.

RGC axon anterograde labeling

To visualize RGC axons in the optic nerve and the brain, 2 μl CTB (2 μg/μl, Invitrogen) was injected into the vitreous body with the same method for AAV injection 2 days before sacrifice.

Retrograde labeling of RGCs

Mice were stabilized in a stereotaxic apparatus after deep anesthesia. A hole was drilled on the skull at 0.5 mm lateral to the sagittal suture and 3 mm posterior to the bregma. 0.5 μl Fluorogold (FG) was injected into the right SC at the depth of 1.6 mm. After injection, mice were kept 10 days before retina harvest.

Intraorbital optic nerve crush

The procedure was similar as previously described (Park et al., 2008). Briefly, the left (ipsilateral) optic nerve was gently exposed by making an incision on the conjunctiva and separating the orbital muscles. The nerve was crushed with jeweler's forceps (Dumont #5; Fine Science Tools) for 2 s approximately 1 mm behind the optic disk.

Pre-chiasm optic nerve crush

The procedure was similar to what has been described previously (Zeng et al., 1995). Briefly, a paramidline incision was made on the scalp. By drilling through the skull, a trapezoid-shaped piece of parietal bone was removed gently. After sucking part of the left frontal lobe by an aspirator, one optic nerve was exposed and crushed by a Domont #5 forceps about 0.5 mm rostral to the optic chiasm. The cavity was washed by cold saline and the incision was sutured. We characterized the complete lesion model by injecting CTB into the vitreous body of the injured eye. No axon could be seen in the chiasm and beyond. FG injection into the SC also did not reveal any labeled cells in the retina. Then mice were kept from 1 to 4 months. The completeness of the lesion in each experimental mouse was verified by anterograde tracing not reaching the SC. Any mice with spared lesion were excluded from further analysis.

Trans-neuronal tracing with PRV

In order to identify the potential reformed circuit by regenerated axons, a recombinant Bartha strain of the pseudorabies virus (PRV) expressing GFP (a gift from Dr. Lynn W. Enquist) was used as a trans-synaptic tracer (Pickard et al., 2002). Briefly, 2 months after the pre-chiasm optic nerve crush, 2 μl PRV-GFP was injected into the anterior chamber of the other intact eye. Mice were sacrificed 96 h after the PRV injection. As previously demonstrated, at this time point, the PRV labeled a restricted set of brain nuclei, the EWN-OPN/IGL/SCN-RGC circuitry, without affecting the integrity of the infected neurons.

Immunofluorescence staining of retina, optic nerve, and brain sections

Mice were given a lethal dose of anesthetic and perfused transcardially with PBS followed by 4% paraformaldehyde (PFA). Eyes, optic nerves and brains were dissected and post-fixed in 4% PFA overnight at 4 °C. Tissues were cryoprotected via increasing concentrations of sucrose. After embedding into OCT compound, the samples were frozen

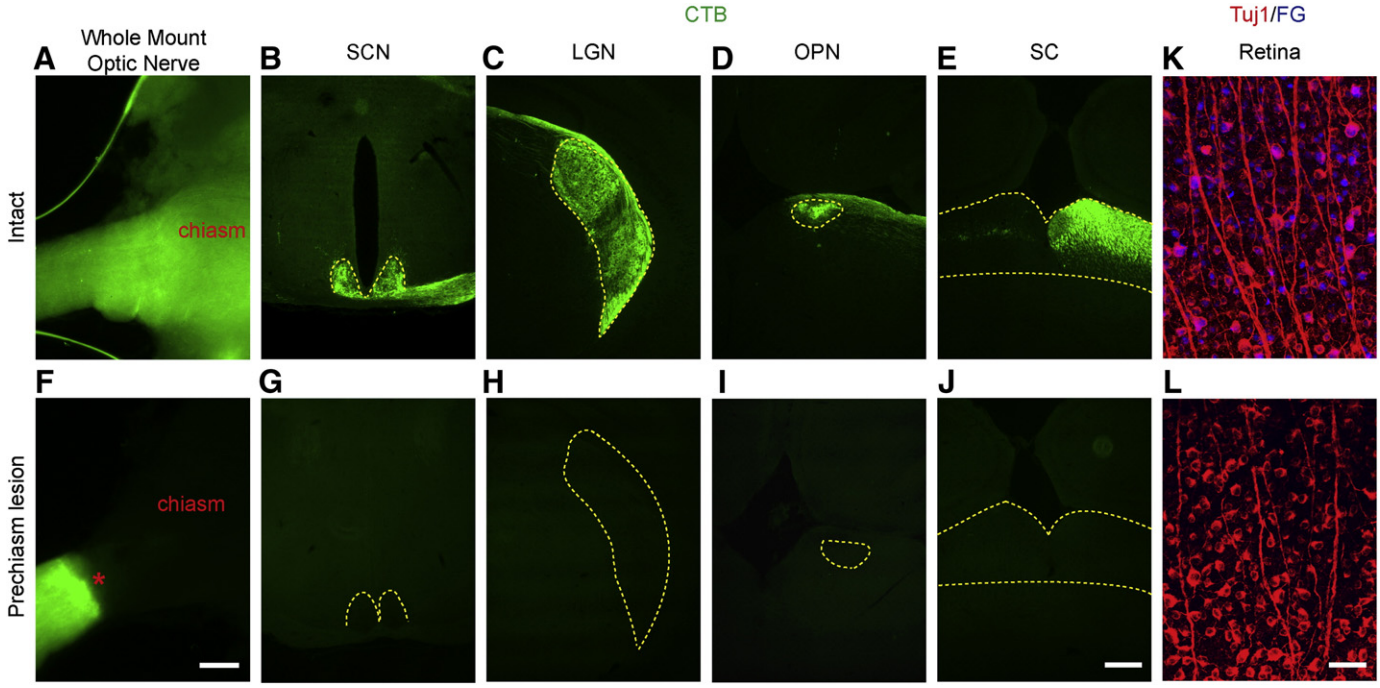

Fig. 2. Characterization of the pre-chiasm optic nerve crush model. (A–J) Representative images of the chiasm, SCN, LGN, OPN, and SC showing CTB labeling in the intact mice (A–E) or in the mice at 1 day after crush (F–J). The asterisk indicates the crush site. The absence of CTB signals along the optic tract and several target nuclei indicated the completeness of the lesion. (K–L) Representative images of the retinas showing Fluorogold (FG) signals after injection into the bilateral superior colliculi in the uninjured mice (K) or in the mice 1 day after pre-chiasm lesion (L). The absence of labeled RGCs in the retina at the side of the lesion also indicated the completeness of the injury. Scale bar: A, F, 100 μm; B–E, G–J, 300 μm; K, L, 50 μm.

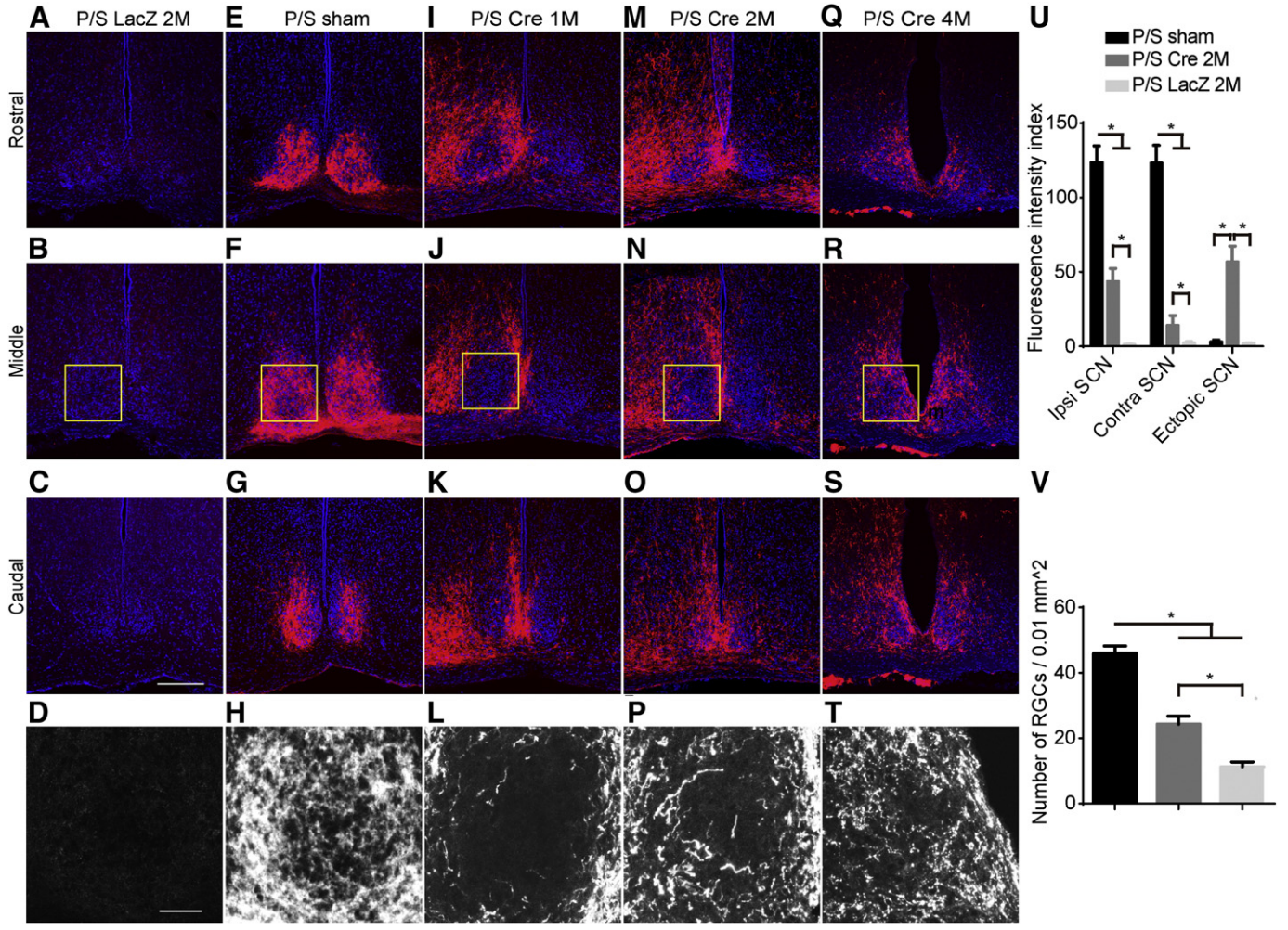

Fig. 3. RGC axons regenerate into the SCN region after pre-chiasm lesion. (A–T) Images of rostral (A, E, I, M, Q), middle (B, F, J, N, R), and caudal (C, G, K, O, S) SCN sections showing CTB-labeled RGC axons (red) in AAV-LacZ injected *Pten*$^{f/f}$;*Socs3*$^{f/f}$ (P/S LacZ) (A–D), sham *Pten*$^{f/f}$;*Socs3*$^{f/f}$ (P/S Sham) (E–H), or AAV-Cre injected *Pten*$^{f/f}$;*Socs3*$^{f/f}$ with CNTF (P/S Cre) (O–T) mice. Scale bar: 200 μm. (A–D) CTB labeling 2 months after lesion in P/S LacZ mice. (I–T) CTB-labeled axons at the SCN region 1, 2 or 4 months after lesion in P/S Cre mice. (D, H, L, P, T) High magnification of boxed area in B, F, J, N, R. Note more bouton-like structures at 4 months. Scale bar: 50 μm. (U) Quantification of CTB labeling intensity at different regions of SCN showing the projection pattern of the regenerating axons at 2 months after lesion. (V) Survival of RGCs at 2 months after lesion. ANOVA, Tukey's post-hoc test, $^{*}P < 0.05$. N = 4–5 mice per group.

by dry ice, and sectioned at −20 °C (25 μm for brains and eye cups, and 8 μm for optic nerves). Immunostaining was performed following standard protocols as follows. All sections were blocked in 4% normal serum and 1% Triton X-100 in PBS for 1 h and incubated in the primary antibodies diluted in the same solution overnight at 4 °C. After being washed three times by PBS, appropriate secondary antibodies (Invitrogen, 1:500) were applied for 1–2 h at RT for single, double or triple staining. After being washed three times, sections were mounted onto glass slides (Superfrost Plus, Fisherbrand) and examined under an epifluorescence (Nikon, TE2000) or confocal microscope (Zeiss, LSM Meta710).

To detect traced axons after intraorbital crush, longitudinal sections of optic nerves and coronal sections of brains were serially collected for anti-CTB staining (List Laboratory). For mice after pre-chiasm crush, coronal sections including SCN, LGN, OPN and SC were collected and examined. VGluT2 (1:500, Millipore) and homer1 (1:500, Synaptic Systems) were used as synaptic markers and staining was done together with CTB to locate newly formed synapses. The number of triple-stained pair of dots was counted and divided by the length of the CTB-labeled axons (per 10 μm). Confocal images were collected for 3-D reconstruction. Isosurfaces were defined separately in the 3 channels with Imagesurfer software to enhance the quality of the reconstructed structure. Hemi-opaque was made for all the channels for a better visualization (Feng et al., 2007). In mice with PRV injection, coronal sections of the brain were stained by anti-GFP (Invitrogen, 1:500). In the SCN, double-staining of CTB and GFP was done to examine the contacts of regrowing axons onto the somata of labeled neurons. Three images of sections containing the labeled SCN neurons were obtained for each animal. The number of contact per neuron was counted in a blind fashion and then averaged. Cross sections of the retina were cut for Tuj1 (1:1000, Covance) and GFP staining.

Immunofluorescence staining of whole-mount retinas

The number of RGCs was determined by whole-mount retina staining. Mouse Tuj1 antibody (1:1000, Covance) was used to detect RGCs. Twelve images (3 for each quarter, spanning the ganglion cell layer of the retina from peripheral to central region) of each retina were captured under the confocal microscope (400×). Manual counting of Tuj1-positive cells was carried by an individual uninformed of assignment to groups.

Quantification of axon profiles in the hypothalamus

In order to analyze the axon innervation pattern in the hypothalamus, confocal images of the SCN region were taken with same program setting and further analyzed by MetaMorph (Molecular Devices). SCN was defined by DAPI staining above the optic chiasm and ectopic SCN

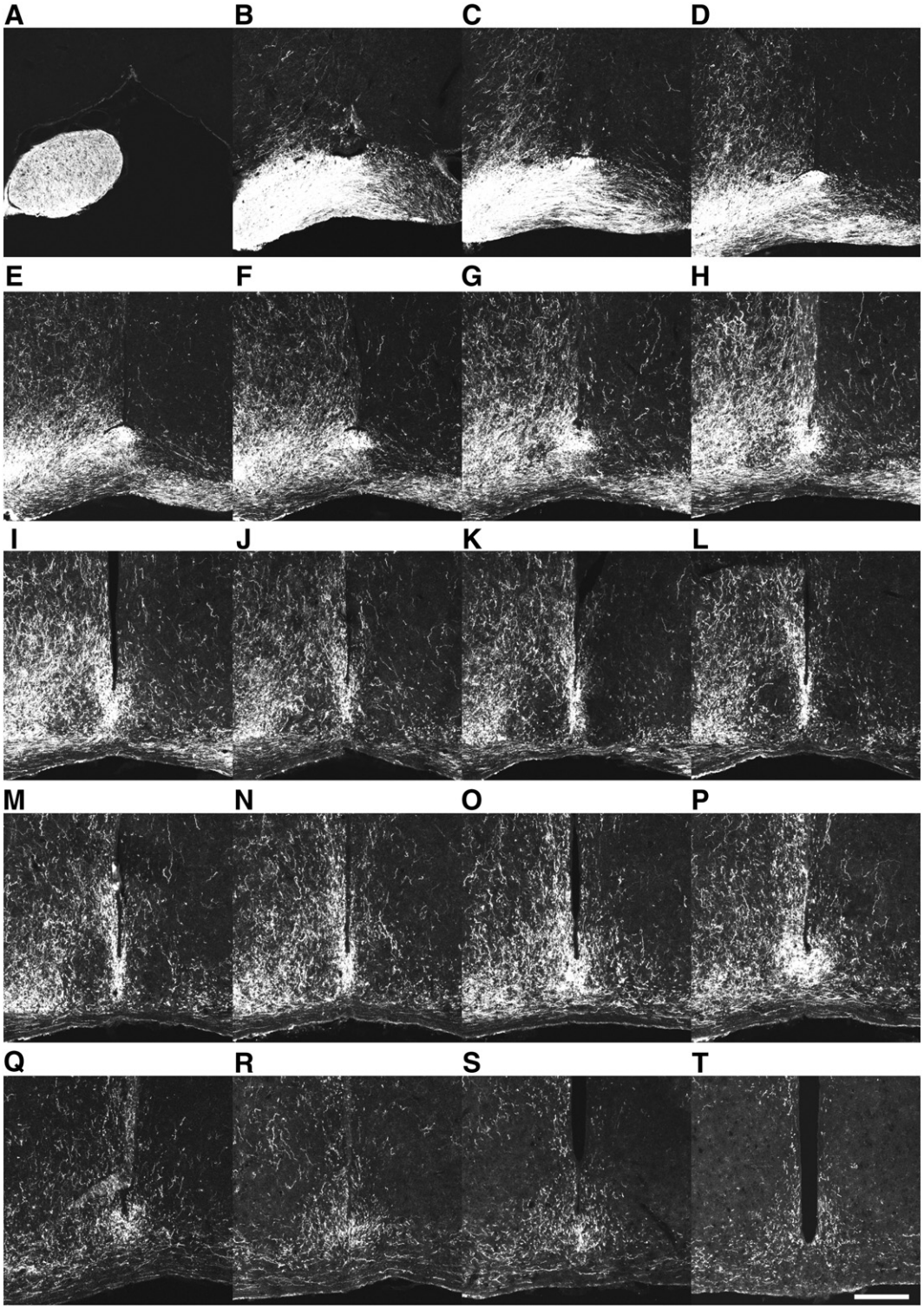

Fig. 4. Serial sections of the hypothalamus with CTB-labeled regenerating axons showing the ectopic projection at 2 months after pre-chiasm lesion. (A) Axons in the optic nerve beyond the crush site. (B–D) Axons at the optic chiasm. Note some axons were not restricted within the chiasm. (E–T) In contrast to the normal intact optic nerve projection, the vast majorities of the axons ectopically innervated the ipsilateral side of the hypothalamus. Except in the rostral (E–I) and caudal (N–P) parts of the oval-shaped nucleus, only a few axons could be seen in the core region of the SCN (J–M). (Q–T) Some axons could be found at the arcuate nucleus. Scale bar: 200 μm.

was defined as a square (150 μm × 150 μm) adjacent to the lateral SCN in hypothalamus. Regions of interest were marked by placing a digital oval (for the SCN), and a digital square (for the ectopic SCN) over the image. Ipsilateral SCN, contralateral SCN and ectopic SCN were measured individually by the sum of all grayscale values divided by the area within the region of interest. Mean background values were obtained from the non-immunoreactive region in the lateral hypothalamus and subtracted from SCN mean gray values. The axon projection

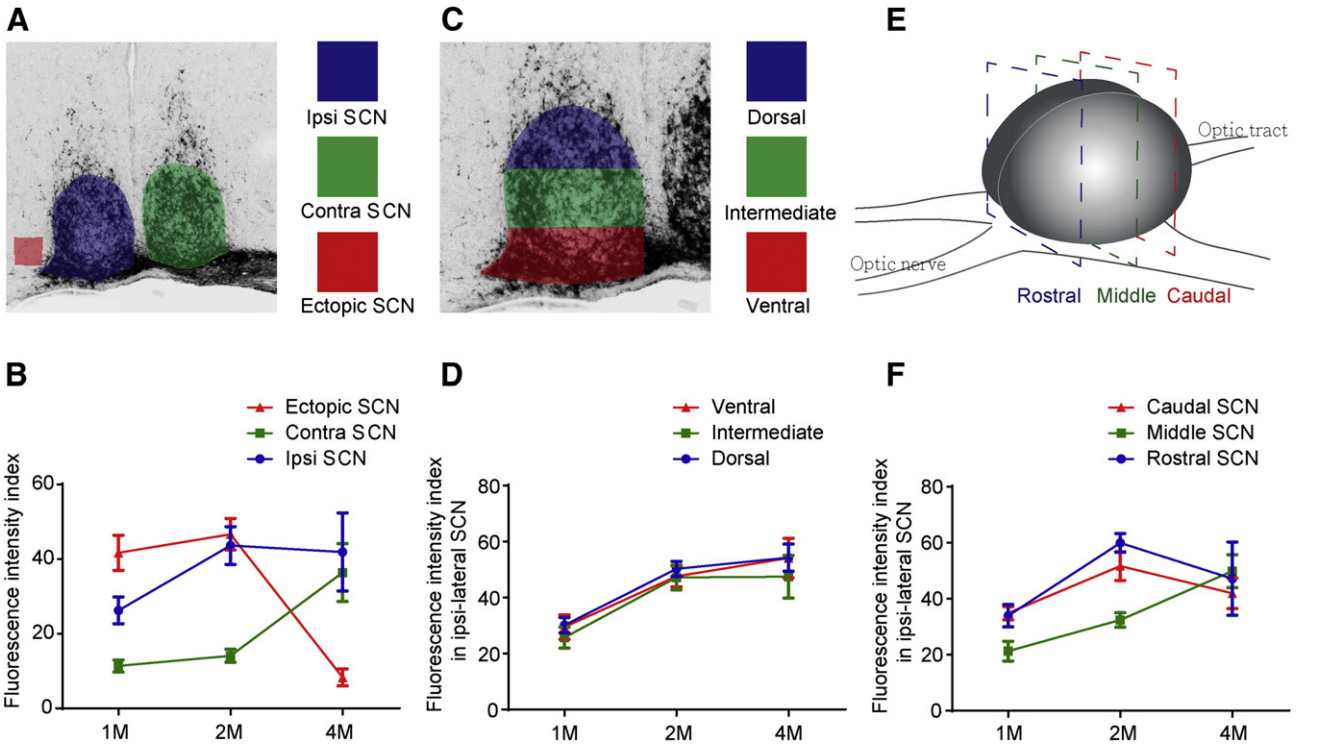

Fig. 5. Spatial and temporal quantification of the RGC axon innervation at the SCN region. (A, B) Quantitation of the CTB-labeling intensity at the ipsilateral, contralateral, and ectopic SCN at different times after injury. At 4 months, many axons pruned from the surrounding region, with more projecting to the contralateral side. (C, D) Quantitation of the CTB-labeling intensity at the ventral, intermediate, and dorsal parts of the ipsilateral SCN at different times after injury. The projections of axons at three parts were similar and increased by time. (E, F) Quantitation of the CTB-labeling intensity at the caudal, middle, and rostral parts of the ipsilateral SCN at different times after injury.

pattern was also analyzed throughout rostral to caudal axis, and dorsal to ventral (vertical) axis within each SCN. To analyze the axon pattern throughout vertical axis, a digital grid was placed over the image to divide the ipsilateral SCN into dorsal, intermediate and ventral parts. At least three coronal sections with SCN were used in each animal.

Transmission electron microscopy

To label the regenerated axons, 2 μl of AAV-GFP was injected intraocularly 1 month after pre-chiasm optic nerve crush. Mice were executed 2 months later by injecting lethal dose anesthetic. SCN was dissected

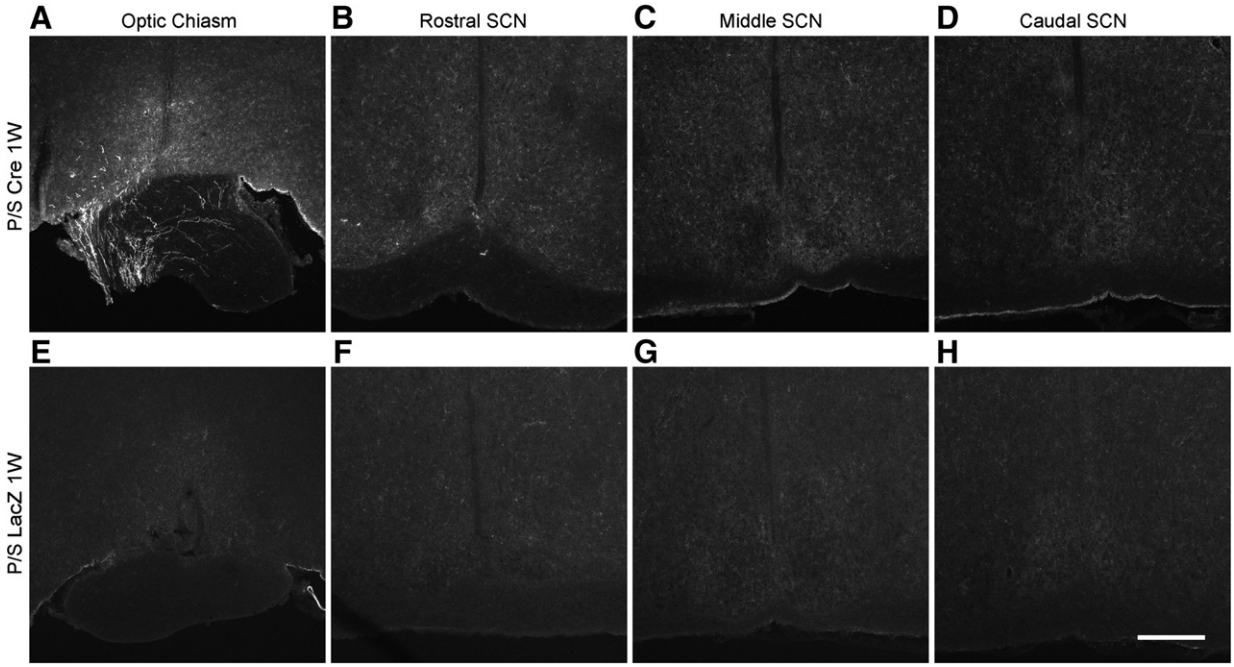

Fig. 6. Regeneration of RGC axons at 1 week after pre-chiasm lesion. (A–D) Images of CTB-labeled RGC axons at 1 week after injury in *Pten*$^{f/f}$;*Socs3*$^{f/f}$ mice injected with AAV-Cre and CNTF. Some axons were observed in the optic chiasm, but not in the SCN area. (E–H) No axons were observed in the brain at 1 week after injury in *Pten*$^{f/f}$;*Socs3*$^{f/f}$ mice injected with AAV-LacZ. Scale bar: 200 μm.

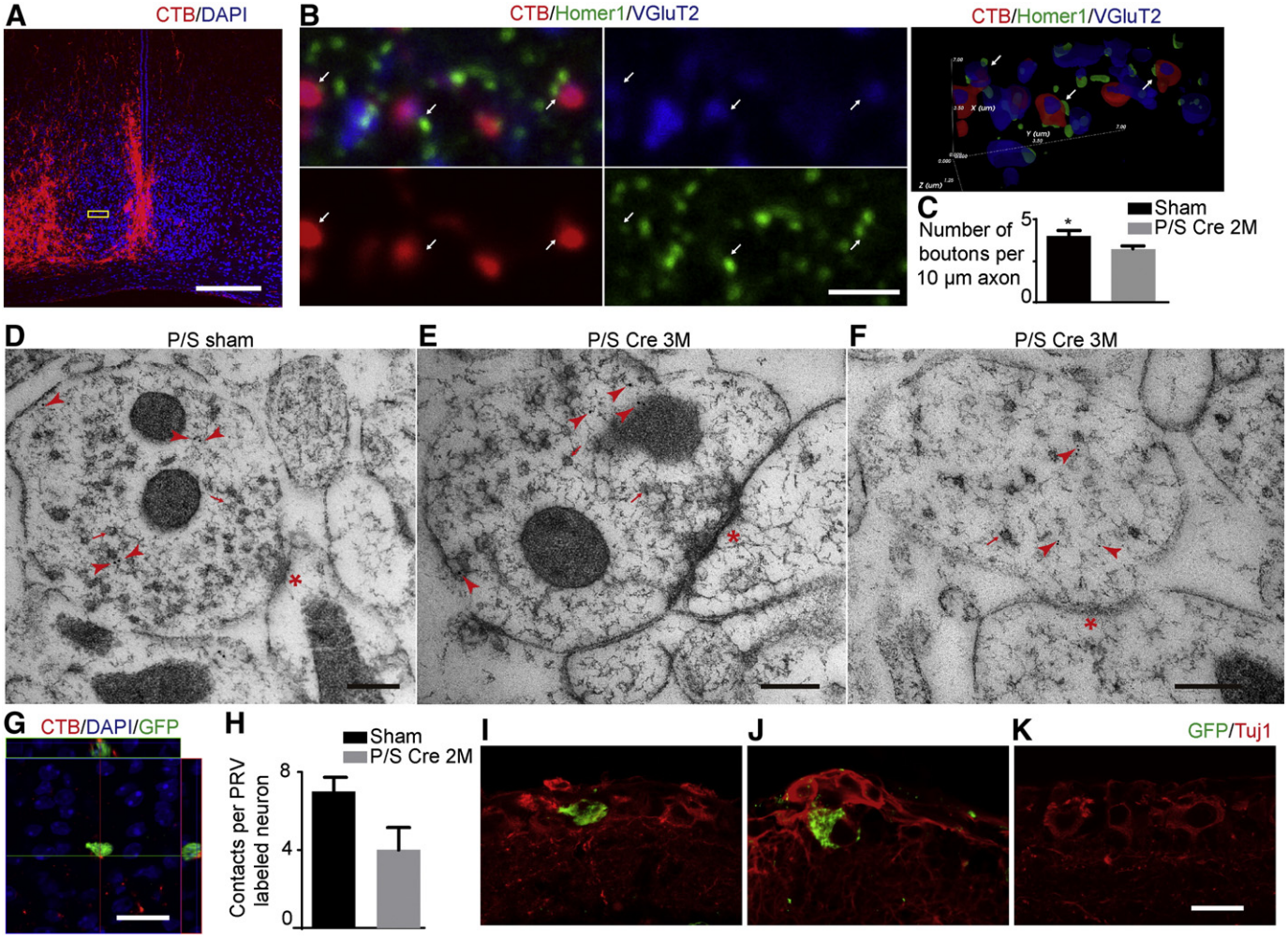

Fig. 7. Regenerating RGC axons reform synaptic connections with SCN neurons. (A) CTB-labeled RGC axons (red) at the SCN 2 months after pre-chiasm lesion. (B) Left: Confocal images by single focal plane scan of CTB-labeled boutons (red) taken at the center of SCN 2 months after pre-chiasm lesion were co-stained with VGluT2 (blue) and Homer1 (green). Arrows point to the triple-labeled synaptic sites. Right: An image after 3-D reconstruction of the confocal image stack. (C) Frequency of boutons in CTB-labeled axons at the core region of SCN in sham control and injured P/S Cre mice. N = 3 mice per group. (D–F) Immunoelectron microscope images showing synaptic structures formed by GFP-labeled RGC axons in the SCN of sham mice (D) and P/S Cre mice 3 months after lesion (E, F). Regenerated synapses resemble the asymmetric synapse from a sham mouse (D) characterized by multiple pre-synaptic vesicles and a prominent post-synaptic density (E). Immature synaptic structures were also observed (F). Arrows, arrowheads, and asterisks indicate synaptic vesicles, gold particles, and synaptic cites respectively. (G) A confocal image showing close contact of boutons (red) from regenerating axons and a GFP-labeled SCN neuron (green) retrogradelly-traced by PRV injection into the contralateral eye 2 months after lesion. (H) Quantification of the contacts in sham mice and injured P/S Cre mice. N = 4 mice per group. (I–K) Representative images of GFP labeling (green) in RGC layers shown by Tuj1 staining (red) of the ipsilateral retinas after PRV injection into the contralateral eyes of the sham mice (I), injured P/S Cre mice (J) and injured P/S LacZ mice (K). Scale bars: A, 200 μm; B, 5 μm; D-F, 200 nm; G, I–K, 20 μm.

and separated into small pieces as quickly as possible before immediately freezing in a high-pressure freezing apparatus (EMP2, Leica). The transmission EM sample preparation and ultra-thin sectioning were performed similarly as described previously (Tse et al., 2004). Immuno-labeling was done by anti-GFP antibody (Invitrogen, 50 μg/ml) and gold-coupled secondary antibody (1:50). Post-stained sections were examined by a Hitachi H-7650 transmission EM with a CCD camera operating at 80 kV.

Light stimulation and c-Fos immunostaining

Light-induced c-Fos activity in SCN was done as previously described (Kornhauser et al., 1990). Briefly, 4 months after pre-chiasm lesion, with the other optic nerve being cut, mice were individually housed in constant darkness (DD) and free-running activity was monitored for 7 days. At subject night (CT16), a white light (100 lx) pulse was turned on. CT12 is defined as the onset of locomotor activity under DD condition. One and half hour after the start of the light pulse, mice were deeply anesthetized and perfused with PFA. Brains were then collected, cryoprotected, frozen, sectioned, and mounted onto slides. Sections were then incubated overnight with the c-Fos antibody (1:1000, Santa Cruz Biotechnology), and visualized with a secondary antibody conjugated with fluorescence tag. Without light stimulation, very few c-Fos-positive cells were observed at SCN in both intact mice and mice with bilateral optic nerve cut, due to endogenous activity. At least 3 images of sections containing the SCN were obtained for each animal. Numbers of immunoreactive cells were counted and then averaged across sections. Counting was performed by an individual uninformed of assignment to groups.

Electrophysiology

Optic nerve evoked EPSCs were done similarly as previously described (Moldavan and Allen, 2010). To prepare brain slices, 2 to 3 months after the pre-chiasm optic nerve crush, mice were anesthetized and decapitated. Brains were quickly dissected and removed to ice-cold Krebs solution consisting of (in mM): 124 NaCl, 26 $NaHCO_3$, 10 glucose, 2.5 KCl, 1.25 NaH_2PO_4, 2 $CaCl_2$, and 2 $MgSO_4$, saturated

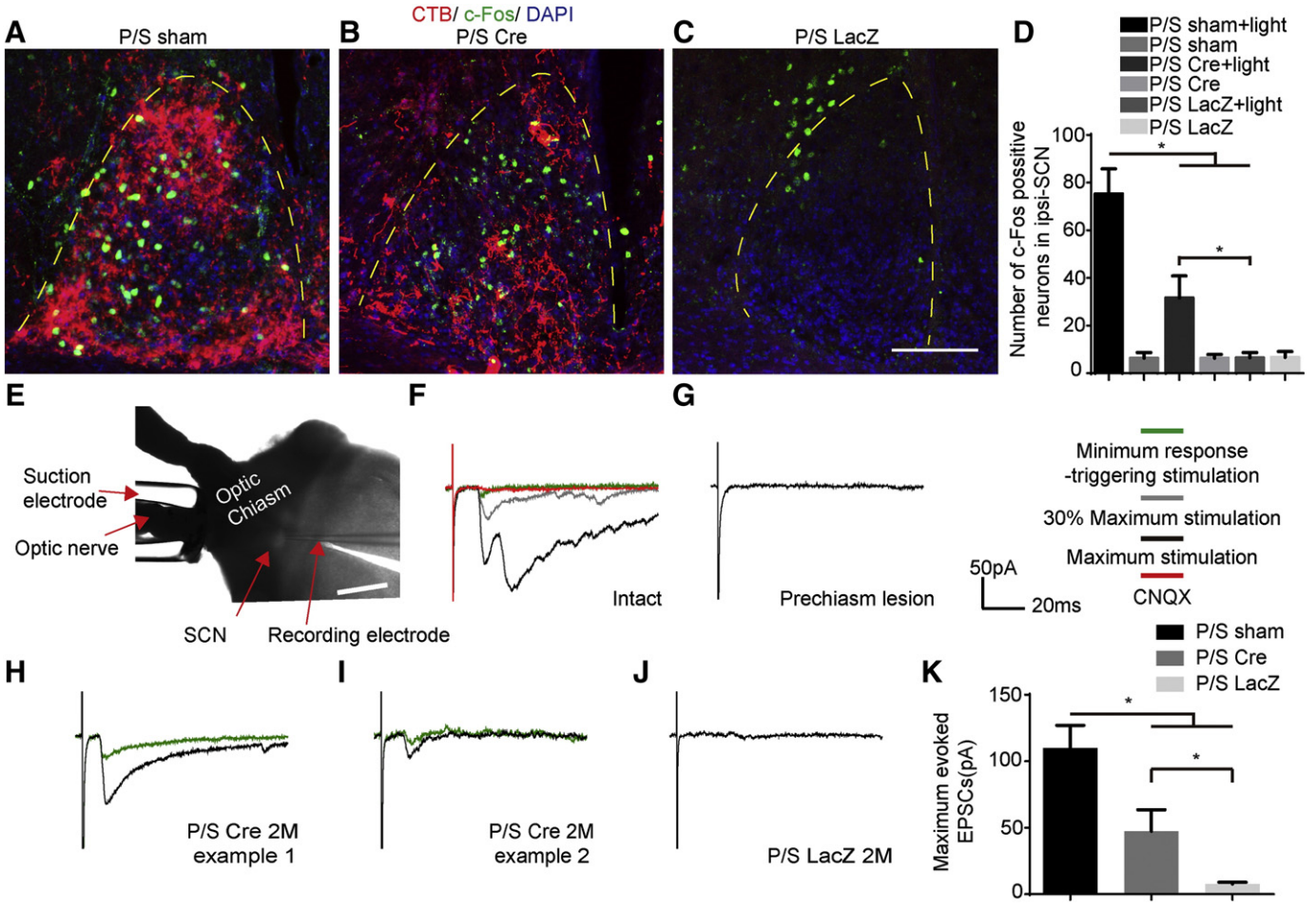

Fig. 8. Stimulation of the regenerating RGC axons induces neuronal activities in SCN neurons. (A–C) Effects of the light pulse administered during subject night (CT16-17) on c-Fos immunoreactivity in the SCN of P/S sham, P/S Cre, and P/S LacZ mice at 4 months after lesion. (D) Number of c-Fos-positive neurons in the SCN. One-way ANOVA, Fisher's LSD post-hoc test, $^*P < 0.05$. N = 3 mice per group. (E) A horizontal hypothalamic slice preparation showing the position of SCN, the stimulating suction electrode, and the recording electrode. Scale bar: 500 μm. (F) Representative evoked post-synaptic current traces of a SCN neuron with increasing stimulus intensities (green, gray, black) and after application of CNQX (red) in sham mice. (G) Evoked EPSCs shortly after pre-chiasm lesion. (H–J) Representative traces of minimum (green) and maximum (black) evoked EPSCs of SCN neurons in the P/S Cre (H, I) and P/S LacZ mice (J) 2 months after injury. (K) Quantification of maximum evoked EPSCs of SCN neurons. One-way ANOVA, Fisher's LSD post-hoc test, $^*P < 0.05$. N = 6–7 mice per group.

with 95% O_2–5% CO_2 (pH 7.4, 295–305 mOsm). One horizontal sections (300–500 μm) containing SCN and optic nerve were obtained with a vibratome (VT 1200 S; Leica Biosystems) and incubated at least 1 h before recording.

For whole-cell recordings, borosilicate glass capillaries were used to prepare microelectrodes with resistances of 6–8 MΩ by a Flaming–Brown horizontal puller (P97; Sutter Instruments) and filled with a solution containing (in mM): 130 CH_3O_3SCs,10 HEPES, 5 NaCl, 1 $MgCl_2$, 0.2 EGTA, 5 QX-314, 2 MgATP, and 0.1 Na-GTP. Whole-cell voltage-clamp recordings were performed with a computer-controlled amplifier (MultiClamp 700B; Molecular Devices), digitized (Digidata1440; Molecular Devices) and acquired with clampex 10.2 (Molecular Devices). The data were filtered at 2 kHz and digitized at 10 kHz. Synaptic responses were recorded in the SCN cells with a suction electrode to stimulate the whole optic nerve. Stimulation pulses (10–40 V; 0.15 mS) were delivered every 15 s. SCN was positioned by morphology under bright field. Patched SCN cells were broken into and voltage-clamped at −70 mV for recording. 6-cyano-7-nitroquinoxaline-2,3-dione (CNQX, 10 μM) was bath applied by perfusion in ACSF containing the final concentration of the compound. The cell was discarded when the input resistance changed more than 30% during the whole cell recording. On average, 5–6 cells were collected for each mouse. Recordings were carried out in mice with unilateral optic nerve crush by an individual uninformed of assignment to groups. Due to technical reasons, we could only reliably do recording in mice up to 5 months old.

Statistical analysis

Student's *t* test was used for the single comparison between two groups. The rest of the data were analyzed using ANOVA. *Post hoc* comparisons were carried out when a main effect showed statistical significance. All analysis was conducted by GraphPad Prism. All bar graphs represent mean ± SEM.

Results

RGC axons reinnervate the SCN region after pre-chiasm lesion with unique projection pattern

Deleting both Pten and Socs3 in retinal ganglion cells (RGCs) by Cre-expressing adeno-associated virus (AAV-Cre) promotes long-distance axonal regeneration after intraorbital crush. Yet, over a 3-month period, we only observed a few axons in the suprachiasmatic nucleus (SCN), the nearest brain target, and none in the lateral geniculate nucleus (LGN), olivary pretectal nucleus (OPN) and superior colliculus (SC) (Fig. 1). This largely agreed with previous findings (Luo et al., 2013), and

prevented us from further pursuit. Then, we managed to crush the optic nerve at the point right before it enters the chiasm (Zeng et al., 1995). We verified the lesion by injecting cholera toxin subunit B conjugated with Alexa-488 (CTB-488) into the vitreous body of the injured eye. Not a single axon could be seen in the chiasm and beyond. Fluorogold (FG) injection into the SC also did not reveal any labeled cells in the retina (Fig. 2). Thus, we established a pre-chiasm optic nerve injury model with complete lesion.

Next, we investigated whether RGC axons can regenerate after pre-chiasmal injury to reinnervate the brain nuclei. AAV-Cre (AAV-LacZ as the control) was injected into the vitreous body of 6–8 week old *Pten*$^{f/f}$;*Socs3*$^{f/f}$ mice, to remove the floxed genes in the RGCs. Three weeks later, we crushed the optic nerve at the point right before it enters the chiasm. We examined the mice at different times post-injury by injecting cholera toxin B (CTB) into the injured eyes to trace axons. In *Pten*$^{f/f}$;*Socs3*$^{f/f}$ mice injected with AAV-LacZ, we did not observe any axons in the brain (Figs. 3A–D). In the AAV-Cre injected mice, at 1 month post-lesion, many axons were located in the chiasm and on both sides of the optic tract, suggesting that some of axons had crossed the midline. In contrast to the normal intact optic nerve projection (Figs. 3E–H), the vast majorities of the axons innervated the ipsilateral side of the hypothalamus, and were not restricted to the SCN. Except in the rostral and caudal parts of the oval-shaped nucleus, few axons could be seen in the core region of the SCN (Figs. 3I–L). At 2 months, serial sections revealed that numerous axons projected into the brain ectopically (Fig. 4). An increasing number of axons were observed at the core region of SCN, with most still maintained around the shell. Some axons started to innervate the contralateral side (Figs. 3M–P). To the best of our knowledge, this is the most extensive re-innervation by regenerating axons into any brain nuclei.

The growth pattern of regenerating axons continuously changed up to 4 months after injury (Figs. 3Q–T). With the total ingrowth temporally decreased, the axons at the core and the ipsilateral SCN had increased (Figs. 3U, 5). The dynamic profiling suggested potential axonal pruning, cell death or both. Indeed, RGC loss occurred after pre-chiasm lesion (Fig. 3V). Several observations suggest that these axons were regenerated rather than spared. First, we only observed significant number of axons in the hypothalamus region beginning at 4 weeks rather than 1 week after injury (Fig. 6). Second, at 4 weeks after injury, axons projected into the ipsilateral hypothalamus including ectopic regions, instead of bilaterally, and largely avoid the core region of SCN. The projection pattern gradually changed over time. Third, in the mice up to three months after lesion, we did not find any axons in the potential targets locating further from the lesion site, such as the OPN and SC (Supplementary Fig. 1). These findings indicate that regenerating RGC axons spontaneously reinnervate the hypothalamus and target part of the SCN within a short distance.

Regenerating retinal axons reform synaptic connections with SCN neurons

Can these axons make synaptic connections with neurons in the hypothalamus? We focused on the SCN, as it is known to be a central circadian regulator (Mohawk et al., 2012), and axons were sharpened at SCN by time. Glutamate has been shown to be the major neurotransmitter for retinal axons projecting to the SCN (Fujiyama et al., 2003). After tracing regenerating axons by CTB 2 months post-injury (Fig. 7A), we used antibodies to label both the pre-synaptic marker vesicular glutamate transporter 2 (VGluT2) and the post-synaptic marker Homer1 — a postsynaptic density (PSD) protein involved in the targeting of glutamate receptors (Dani et al., 2010). Many pairs of dots with triple staining were found at the SCN by confocal imaging and 3-D reconstruction, indicating that they were potentially excitatory synaptic sites (Figs. 7B–C).

To obtain definitive evidence of synapse formation, we over-expressed GFP in the regenerating axons through AAV 7 weeks after pre-chiasm injury, and assessed whether they formed synapses at the ultrastructural level 6 weeks after injection. We performed immunogold transmission electron microscopy (TEM) on ultrathin sections prepared from high-pressure frozen/freeze-substituted SCN, and labeled by GFP antibodies. We found some structures with key features of pre-injured asymmetric synapses (Fig. 7D): a contact zone accumulated with pre-synaptic vesicles and a PSD (Fig. 7E). We also noticed that some had few vesicles in the terminal and close apposition of pre- and post-synaptic membranes that do not yet display a PSD (Fig. 7F), suggesting that they were potentially newly formed or immature synapses. These results indicate that regenerating retinal axons possess the ability to reform synapses in the SCN.

Regenerating optic nerve integrates with a neuronal circuitry

Because the observed regenerating axons were mostly restricted at the shell, but not in the core region of the SCN, we wondered whether they had integrated into the existing brain circuitry. To trace SCN-projecting RGCs, we used a recombinant Bartha strain of the pseudorabies virus (PRV) that expresses GFP and exclusively spreads trans-neuronally in the retrograde direction (Pickard et al., 2002). As the simplified spreading scheme in intact mice revealed (Supplementary Fig. 2), via autonomic circuits to the eye, PRV injected into the anterior chamber of the eye retrogradely infects specific retinorecipient nuclei in the brain, namely the OPN, intergeniculate leaflet (IGL) and the SCN, resulting in labeled ganglion cells in the other retina 96 h after intraocular infection (Pickard et al., 2002). Seven weeks after pre-chiasm lesion, we injected PRV into the contralateral non-injured eye. Some bouton-like structures could be seen from the regenerating axons onto the somata of PRV-labeled SCN neurons (Fig. 7G), at about half of the rate in intact mice (Fig. 7H). Some RGCs in the ipsilateral lesioned eye were labeled only in the sham (Fig. 7I) and regenerated mice (Fig. 7J), but not in the injured control (Fig. 7K). Because the regenerating axons did not reach the OPN, and rarely the IGL, the labeling could largely come from the axonal projection into the SCN. Based on the evidence of synapse formation in the SCN and PRV labeling in RGCs, it is very likely that regenerating axons connect with part of the brain circuitry by projecting back to the SCN.

Photic or electric stimulation of retinal axons induces post-synaptic activities in SCN neurons

Next, we assessed whether these new synaptic connections in the SCN were active using either optical or electrical stimulation. Light regulates c-Fos gene expression in SCN neurons through retinal projection (Kornhauser et al., 1990). Four months after pre-chiasmal lesioning, we cut the contralateral optic nerve, placed the mice under constant darkness, and monitored each individual's free-running activity. A light pulse during subjective night (CT16-17) induced more c-Fos-positive cells within the SCN in regenerated mice, than in the injured controls (Figs. 8A–D). To demonstrate the post-synaptic neuronal response directly, we performed the whole-cell patch clamp recordings of SCN neurons with optic nerve stimulation in acute brain slices (Moldavan and Allen, 2010) (Fig. 8E). Evoked EPSCs were readily detected in intact animals, and were nearly abolished by the application of the AMPA antagonist CNQX (Fig. 8F), indicating that the responses were through glutamatergic synaptic transmission. We rarely detected any evoked responses in the injured controls (Figs. 8G, J). In contrast, we could record evoked EPSCs in some of the neurons in the regenerated mice 2 months after lesion (Figs. 8H, I) with smaller current amplitudes compared with their intact counterparts (Fig. 8K), possibly due to limited axonal convergence onto the recorded neurons or immaturity of the synapses. These results imply that stimulations induce neuronal activity through reformed excitatory synaptic connections.

Discussion

As expected, *Pten* and *Socs3* co-deletion promotes robust RGC axon regeneration to cross the lesion site after pre-chiasm lesion, although the lesion locates at a distance 6–7 mm further away from the eye compared to the intraorbital crush. In a few weeks, we observed very extensive hypothalamus innervation. To our surprise, axons appear to overgrow initially, then spontaneously restructure by time. Importantly, regenerating axons converge onto SCN neurons that connect with an existing brain circuitry, and reform glutamatergic excitatory synapses. Albeit not completely normal, either physiological or electrical stimulations evoke post-synaptic neuronal responses. Thus, robust regeneration into natural targets and functionally active synapses can be experimentally induced at the same time after adult CNS injury by only manipulating intrinsic mechanisms.

Recently, it has been demonstrated that conditioning lesion combined with neurotrophin-3 (NT-3) delivery promotes sensory axons to reinnervate the nucleus gracilis after a C1 spinal cord lesion but not a C4 lesion (Alto et al., 2009), suggesting that long distance in the inhibitory environment could be a limiting factor for successful rewiring back to the original target. Here we showed that, within a few mm range, retinal axons grow into the hypothalamus extensively. The innervation does not seem to be completely random since the core region of the SCN is largely avoided initially, suggesting that regenerating axons respond to potential local cues. During development, the coordinated expression of specific transcription factors and guidance receptors in RGCs and guidance cues in the ventral diencephalon influences RGC axon guidance for midline crossing (Petros et al., 2008). It will be interesting to assess whether similar mechanisms regulate the axon innervation in the pre-chiasm lesion model.

Our results also indicate that many axons overgrow into ectopic regions and are gradually eliminated from the hypothalamus. It raises questions whether axons prune from ectopic regions due to lack of active connections or those ectopically projecting neurons are dying due to lesion. Preventing apoptosis such as by knocking out Bax in RGCs may help to distinguish the two possibilities (Jiao et al., 2005). Nevertheless, SCN-innervating axons persist up to 4 months after injury and form synapse with target neurons. In normal mice, the SCN receives axons predominantly from M1 and M2 intrinsically photosensitive RGCs (ipRGCs) that express photopigment melanopsin (Schmidt et al., 2011). These ipRGCs play a major role in synchronizing circadian rhythms to the light/dark cycle by projecting into SCN (Berson et al., 2002; Hattar et al., 2002). It will be informative to find out to what extent that the SCN-innervating axons are derived from the ipRGCs.

Corticospinal tract axons cross the lesion after deleting *Pten* and form synapses at the distal cord (Liu et al., 2010). However, we cannot assume that reformed synapses, even they exist, will naturally be active. For example, lesioned dorsal root ganglion axons reinnervate and form synapses in the nucleus gracilis by combining conditioning lesion and NT-3. But stimulation of the sciatic nerve cannot evoke post-synaptic responses (Alto et al., 2009). Here we provide evidence that regenerating axons form synapses with circuitry-integrating SCN neurons, and post-synaptic neuronal responses are induced by stimulations. Due to technical difficulties, we can only consistently perform brain slice recording in mice up to 5 months old, 2 months after lesion. Evoked post-synaptic EPSCs are much smaller than the ones recorded in the sham mice, consistent with our findings that SCN neurons receive fewer retinal axon contacts than normal, and the existence of immature synapses. Our results suggest that understanding mechanisms regulating synaptic formation by regenerating axons is an important future direction in order to promote rewiring to potential functional repair.

Conclusions

Taken together, the immunofluorescence labeling, trans-neuronal tracing, ultrastructural analysis, and electrophysiological results indicate that adult retinal axons with *Pten* and *Socs3* co-deletion not only have the ability to regenerate, but also to find the path to innervate their nature target, and make active connections with SCN neurons. The axon innervation, dynamic axon restructuring, and ongoing maturation of synapses suggest that the regenerating axons may reproduce many features of retinal axons during development (Hooks and Chen, 2006) and functional regeneration in lower vertebrates (Beazley et al., 2003; Schmidt, 1985), suggesting that similar mechanisms may regulate axon rewiring in injured adult mammalian. Both the innervation pattern and evoked responses by the regenerating axons are not completely normal, suggesting that combining with other strategies is necessary to overcome the defective rewiring. Further understanding of this simple and reproducible pre-chiasm lesion model can help us to tackle more complicated rewiring failures after CNS injury.

Supplementary data to this article can be found online at http://dx.doi.org/10.1016/j.nbd.2014.09.019.

Acknowledgments

We are grateful to Dr. Lynn W. Enquist (Princeton University, NJ, USA) for the generous gift of PRVs. We also thank Dr. Karl Herrup for critical reading of the manuscript. This study was supported in part by the Hong Kong Research Grants Council Theme-based Research Scheme (T13-607/12R), the National Key Basic Research Program of China (2013CB530900), the Research Grants Council of Hong Kong SAR (AoE/M-09/12, HKUST662011, HKUST662012, HKUST6 89913, HKUST5/CRF/12R, CUHK2/CRF/11G and AoE/M-05/12), and the Hong Kong SCI Foundation.

References

Aguayo, A.J., et al., 1981. Influences of the glial environment on the elongation of axons after injury: transplantation studies in adult rodents. J. Exp. Biol. 95, 231–240.
Alto, L.T., et al., 2009. Chemotropic guidance facilitates axonal regeneration and synapse formation after spinal cord injury. Nat. Neurosci. 12, 1106–1113.
Beazley, L.D., et al., 2003. Training on a visual task improves the outcome of optic nerve regeneration. J. Neurotrauma 20, 1263–1270.
Berson, D.M., et al., 2002. Phototransduction by retinal ganglion cells that set the circadian clock. Science 295, 1070–1073.
Bradke, F., et al., 2012. Assembly of a new growth cone after axotomy: the precursor to axon regeneration. Nat. Rev. Neurosci. 13, 183–193.
Carter, D.A., et al., 1989. Regenerated retinal ganglion cell axons can form well-differentiated synapses in the superior colliculus of adult hamsters. J. Neurosci. 9, 4042–4050.
Dani, A., et al., 2010. Superresolution imaging of chemical synapses in the brain. Neuron 68, 843–856.
de Lima, S., et al., 2012. Full-length axon regeneration in the adult mouse optic nerve and partial recovery of simple visual behaviors. Proc. Natl. Acad. Sci. U. S. A. 109, 9149–9154.
Dickendesher, T.L., et al., 2013. NgR1 and NgR3 are receptors for chondroitin sulfate proteoglycans. Nat. Neurosci. 15, 703–712.
Feng, D., et al., 2007. Stepping into the third dimension. J. Neurosci. 27, 12757–12760.
Filbin, M.T., 2006. Recapitulate development to promote axonal regeneration: good or bad approach? Philos. Trans. R. Soc. Lond. B Biol. Sci. 361, 1565–1574.
Fujiyama, F., et al., 2003. Changes of immunocytochemical localization of vesicular glutamate transporters in the rat visual system after the retinofugal denervation. J. Comp. Neurol. 465, 234–249.
Giger, R.J., et al., 2010. Guidance molecules in axon regeneration. Cold Spring Harb. Perspect. Biol. 2, a001867.
Harel, N.Y., Strittmatter, S.M., 2006. Can regenerating axons recapitulate developmental guidance during recovery from spinal cord injury? Nat. Rev. Neurosci. 7, 603–616.
Hattar, S., et al., 2002. Melanopsin-containing retinal ganglion cells: architecture, projections, and intrinsic photosensitivity. Science 295, 1065–1070.
Hooks, B.M., Chen, C., 2006. Distinct roles for spontaneous and visual activity in remodeling of the retinogeniculate synapse. Neuron 52, 281–291.
Jiao, J., et al., 2005. Bcl-2 enhances Ca(2+) signaling to support the intrinsic regenerative capacity of CNS axons. EMBO J. 24, 1068–1078.
Keirstead, S.A., et al., 1989. Electrophysiologic responses in hamster superior colliculus evoked by regenerating retinal axons. Science 246, 255–257.
Kornhauser, J.M., et al., 1990. Photic and circadian regulation of c-fos gene expression in the hamster suprachiasmatic nucleus. Neuron 5, 127–134.
Leon, S., et al., 2000. Lens injury stimulates axon regeneration in the mature rat optic nerve. J. Neurosci. 20, 4615–4626.
Liu, K., et al., 2010. PTEN deletion enhances the regenerative ability of adult corticospinal neurons. Nat. Neurosci. 13, 1075–1081.

Liu, K., et al., 2011. Neuronal intrinsic mechanisms of axon regeneration. Annu. Rev. Neurosci. 34, 131–152.
Luo, X., et al., 2013. Three-dimensional evaluation of retinal ganglion cell axon regeneration and pathfinding in whole mouse tissue after injury. Exp. Neurol. 247, 653–662.
Mohawk, J.A., et al., 2012. Central and peripheral circadian clocks in mammals. Annu. Rev. Neurosci. 35, 445–462.
Moldavan, M.G., Allen, C.N., 2010. Retinohypothalamic tract synapses in the rat suprachiasmatic nucleus demonstrate short-term synaptic plasticity. J. Neurophysiol. 103, 2390–2399.
Moore, D.L., et al., 2009. KLF family members regulate intrinsic axon regeneration ability. Science 326, 298–301.
Park, K.K., et al., 2008. Promoting axon regeneration in the adult CNS by modulation of the PTEN/mTOR pathway. Science 322, 963–966.
Petros, T.J., et al., 2008. Retinal axon growth at the optic chiasm: to cross or not to cross. Annu. Rev. Neurosci. 31, 295–315.
Pickard, G.E., et al., 2002. Intravitreal injection of the attenuated pseudorabies virus PRV Bartha results in infection of the hamster suprachiasmatic nucleus only by retrograde transsynaptic transport via autonomic circuits. J. Neurosci. 22, 2701–2710.
Schmidt, J.T., 1985. Formation of retinotopic connections: selective stabilization by an activity-dependent mechanism. Cell. Mol. Neurobiol. 5, 65–84.
Schmidt, T.M., et al., 2011. Intrinsically photosensitive retinal ganglion cells: many subtypes, diverse functions. Trends Neurosci. 34, 572–580.
Schwab, M.E., Bartholdi, D., 1996. Degeneration and regeneration of axons in the lesioned spinal cord. Physiol. Rev. 76, 319–370.
Smith, P.D., et al., 2009. SOCS3 deletion promotes optic nerve regeneration in vivo. Neuron 64, 617–623.
Sun, F., et al., 2011. Sustained axon regeneration induced by co-deletion of PTEN and SOCS3. Nature 480, 372–375.
Tse, Y.C., et al., 2004. Identification of multivesicular bodies as prevacuolar compartments in *Nicotiana tabacum* BY-2 cells. Plant Cell 16, 672–693.
Winzeler, A.M., et al., 2011. The lipid sulfatide is a novel myelin-associated inhibitor of CNS axon outgrowth. J. Neurosci. 31, 6481–6492.
Zeng, B.Y., et al., 1995. Regenerative and other responses to injury in the retinal stump of the optic nerve in adult albino rats: transection of the intracranial optic nerve. J. Anat. 186 (Pt 3), 495–508.
Zheng, B., et al., 2006. Genetic mouse models for studying inhibitors of spinal axon regeneration. Trends Neurosci. 29, 640–646.